Nano-Structures & Nano-Objects 12 (2017) 46–56

Contents lists available at ScienceDirect

Nano-Structures & Nano-Objects

journal homepage: www.elsevier.com/locate/nanoso

Evolution of ternary I–III–VI QDs: Synthesis, characterization and application

Ncediwe Tsolekile [a,b,c], Sundararajan Parani [a,b], Mangaka C. Matoetoe [c], Sandile P. Songca [d], Oluwatobi S. Oluwafemi [a,b,*]

[a] Department of Applied Chemistry, University of Johannesburg, P.O. Box 17011, Doornfontein 2028, Johannesburg, South Africa
[b] Centre for Nanomaterials Science Research, University of Johannesburg, Johannesburg, South Africa
[c] Department of Chemistry, Cape Peninsula University of Technology, P.O. Box 652, Cape Town 2000, South Africa
[d] Department of Chemistry, University of Zululand, PB X1001, Kwadlangezwa, 3886, South Africa

GRAPHICAL ABSTRACT

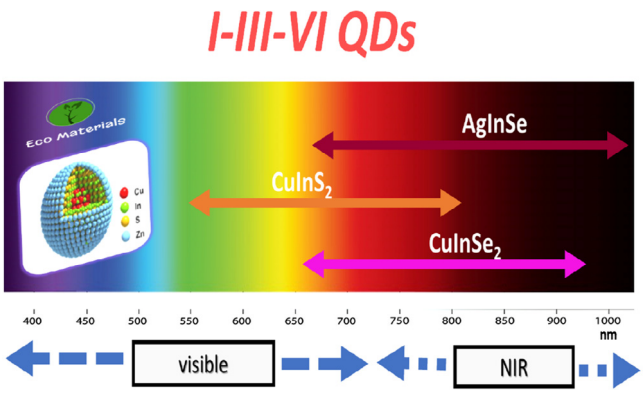

ARTICLE INFO

Article history:
Received 9 July 2017
Received in revised form 19 August 2017
Accepted 25 August 2017

Keywords:
Quantum dots
Copper indium sulphide
Synthesis
Conjugation
Cytotoxicity
Bio-imaging

ABSTRACT

The paradigm-shift in quantum dot (QDs) synthesis and applications in the past decade have seen the development of an array of semiconductor QDs. The II–VI or IV–VI QDs are still the most researched QDs undoubtedly. However, safer alternatives within the ternary I–III–VI QDs are currently being pursued. This has resulted in an increased new body of knowledge on nanomaterial technology. This paper reviews the evolution of synthetic methods for I–III–VI QDs and their surface modification techniques with a particular focus on the ternary copper-indium-sulphide (CIS) based QDs. The parameters that play a vital role in the optical properties of CIS QDs, and their various applications with emphasis on biological applications are also discussed. The review ends with the challenge and future perspective of these nascent QDs.

Contents

* Corresponding author at: Department of Applied Chemistry, University of Johannesburg, P.O. Box 17011, Doornfontein 2028, Johannesburg, South Africa.
E-mail address: oluwafemi.oluwatobi@gmail.com (O.S. Oluwafemi).

http://dx.doi.org/10.1016/j.nanoso.2017.08.012
2352-507X/

1. Introduction

Since their origin in the late 1980's, quantum dots (QDs) has been a central theme in nanotechnology. QDs are nano-crystalline fluorescent semiconductors that confines the motion of their charge carriers in three dimensions [1]. For a material to be considered as "quantum dots", stern confinement of electron to hole with a radius equal to or below the exciton Bohr radius is required [2]. QDs are intermediate state of matter with average diameters of 2–20 nm that display properties that is not present neither in the bulk nor molecular systems. Altering their size by the addition or subtraction of just a few atoms to the quantum dots has the effect of altering the boundaries of the bandgap. Depending on the bandgap, the excited QDs emits photons at different wavelengths [3]. They emit from the visible to NIR region as their size increases.

QDs have been extensively investigated for diverse applications due to their unique properties such as size-dependent optical properties, broad excitation spectra, narrow bandwidth emission spectra, high resistance to photo-bleaching, good stability and biocompatibility. These salient features have resulted in the exploration of QDs as potential alternatives to conventional organic fluorophores for biomedical and analytical applications such as bio-labelling and imaging, bioassay, drug delivery, photodynamic therapy (PDT), biosensor and chemosensor, to mention a few [4]. Traditionally, QDs are typically prepared as binary semiconductor nanocrystals from group II–VI (e.g. CdSe, ZnS etc.) and group IV–VI elements (e.g. PbTe, PbS) in the periodic table. Cadmium(Cd) based QDs are the most studied owing to their excellent optical properties [5] which have guided research on the use of QDs. Much work has been done using these QDs in various applications such as medicine [6], electronics [7,8] and other industries. Though these materials possess excellent properties, the use of these II–VI and IV–VI QDs is limited due to the inherent toxicity of heavy metals such as Cd and Pb. Even though encapsulation of these QDs with different shells such as silica, polymers and so on significantly reduces the leakage of heavy metals from the core, it is not deniable that, these QDs contain potential hazards, which are harmful to the biological system and the environment [6].

Recent works have deviated from the use of these toxic metals particularly in biomedical fields where QDs utility is limited due to their cytotoxicity. Growing interest has been on the chalcopyrite ternary QDs from I–III–VI group [7,9]. The QDs that have been investigated within the I–III–VI group are $CuInS_2$ (CIS), $CuGaS_2$ (CGS), $AgInS_2$ (AIS), AgInSe (AISe) and $AgGaS_2$ (AGS) [7,10–12]. It is worth noting that, among these QDs, much attention has been given to CIS QDs [13]. The vast colour window up to NIR range (850 nm), direct band gap, large Stokes shift, long fluorescence lifetime and most importantly the absence of toxic elements [7] are some of the advantages of using CIS QDs. Herein, we review the recent literature regarding the preparation of ternary QDs with particular focus on CIS QDs and their most important properties. Their surface modifications and applications are also discussed with focus on biological application.

2. Synthetic strategies

Different methods have been reported for the synthesis of QDs. Selection of the synthetic approach is widely dependent on the desired use of the QDs and the type of solvents. Synthesis of CIS ternary QDs is reported to be intricate due to the reactivity of the cations commonly used (Cu^{2+}, In^{3+}, and Zn^{2+}) [14]. Furthermore, the synthesis is also limited by the shape, composition and size control due to multifaceted equilibria that occurs between the cation and anion precursor reactivity's [15]. However, tuning of reaction parameters such as temperature, reaction time and precursor ratios allows for the attainment of mono-dispersed size controlled quantum dots.

For sulphur based ternary QDs such as CIS, the sulphur sources are often stabilizing ligands such as dodecane thiol (DDT), mercapto-propionic acid (MPA), glutathione (GSH), thioglycolic acid (TGA) [11,16,17]. These ligands undergo thiolysis to supply enough sulphur ions and bind to the surface of the QDs thereby performing dual role in the synthesis [18–20]. Numerous studies have reported the synthesis of CIS QDs under similar reaction conditions of temperature, pH, reactant concentration and ratio, but different stabilizing agents and, this had produced different results. To balance the reactivity's of Cu^{+} and In^{3+}, two stabilizing agents are often used in the synthesis of CIS QDs [21].

The optical properties of the QDs majorly lie within the spherical core. However, core based QDs such as CIS QDs have been reported to lose their properties with time mainly because of their high reactivity (due to their large surface area to volume ratio)

which also causes surface defects. Therefore, during the synthesis, coating the QDs surface with another semiconductor material to form core/shell type QDs is generally employed to reduce the surface defects [22]. ZnS is the most commonly used shell material because of its higher band gap [23,24] in order to improve the quantum yield and enhance the photo-stability by passivating the surface of the QDs [17,25]. ZnS (3.7 eV) has a higher band gap than CIS (1.45 eV) and exhibits a type I core/shell CIS/ZnS QDs [26]. This allows for the exciton confinement of the core by reducing surface-related recombination in trap states [27]. CIS chalcopyrite crystal structure is the superstructure of zinc blende like ZnS structure. The low lattice mismatch between CIS and ZnS allows for the epitaxial growth of ZnS on CIS with the minimum strain at the core/shell interface [15,28]. Several authors have reported the blue-shift that occurs during the growth of ZnS over CIS QDs [15, 29,30] and this has been attributed to the cation exchange of Cu^{+} and In^{3+} ions with Zn^{2+} ions. This is feasible due to their similar ionic radii and Gibbs formation, which allows for cation exchange. The other possible reasons that have been suggested for the blue-shift which occurs during shelling are the inter-diffusion of Zn atoms, surface reconstruction and etching of the plain core material [31]. Kim et al., 2017 [32] reported on the tuning of Cu:In ratio along with variation in reaction temperature and time in order to address the blue-shifting that occurs during the ZnS growth. Their results showed that the degree of passivation by the ZnS shell at different synthesis temperatures results in a PL quantum yield (QY) of between 26%–38%. The cation exchange and blue shifting of the emission position were inhibited when the reaction was temperature was 180 °C. However, the PL spectra becomes blue-shifted proportionally as the synthesis time increased. The formation of zinc alloyed CIS QDs prior to forming core/shell have been reported to reduce the blue-shift during shelling whereby, a Zn^{2+} precursor is added at the beginning of the reaction to alloy with the Cu^{+} and In^{3+} [26,33]. This has also been reported to inhibit any structural defects in the core [26,34,35].

2.1. Organic synthesis

The basic principle of organic synthesis involves the pyrolysis of organometallic precursors in hydrophobic solvents and ligands at high boiling temperatures (typically between 220 and 300 °C) under inert atmosphere. Organic synthesis produces high-quality colloidal nanoparticles often generated using precursors in the presence of hydrophobic reducing agents and/ or ligands such as octadecene (ODE), 1-dodecanethiol (DDT), octylamine (OctAm), oleylamine (OlAm), tri-octylphosphine oxide (TOPO) [15]. These ligands passivate the surface of QDs, which renders them hydrophobic. There are different methods of synthesizing CIS QDs in organic medium, which includes hot-injection method, solvothermal, thermolysis and the heating up method. The following section gives a brief description on the synthesis methods.

2.1.1. Hot-injection method

The hot-injection method involves the injection of a cool solution of the anionic precursor into a hot solution of cationic precursor at high temperature followed by fast nucleation. (Fig. 1). It also permits control of the particle size distribution [36]. Vahidshad et al., 2013 [37] synthesized CIS nanocrystals using CuCl, $InCl_3$ and thiourea as precursors. The size of the nanocrystals was tuned by varying the injection temperature between 150 and 270 °C. The result showed that high reaction temperatures resulted in fast nucleation followed by slower particle growth compared to lower temperatures. The optimized temperature for instant injection was 240 °C for CIS. By tuning and controlling the solution temperature, injection rate and coordinating solvent to capping agent ratio they were able to synthesize material with narrow size distribution

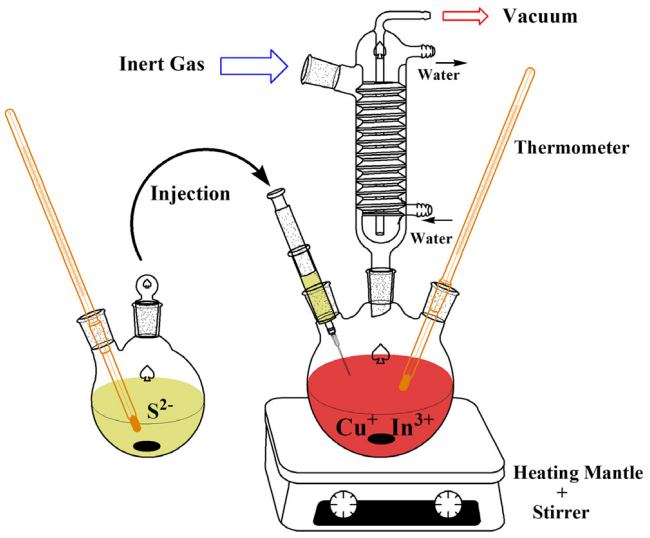

Fig. 1. Schematic representation of organic synthesis. Vahidshad et al., 2013 [37].

and particle diameters between 10 and 30 nm. The study also emphasized the importance of injection temperature with respect to hot-injection method. Yuan et al., 2010 [38] however, advised against the use of the injection method for large volumes as injection process can be slowed down. Thus, causing overlap between nucleation and growth, which can lead to unwanted broad particle size distributions.

2.1.2. Solvothermal

The solvothermal method is known for its facile and large-scale up properties. It is, therefore, an advantageous method for the production I–III–VI type QDs at gram scale. The solvothermal method initially involves the combination of anionic and cationic precursors at lower temperatures. For desired particle growth with good crystallinity, the temperature is later increased with the use of an autoclave [39,40]. Nam et al., 2011 [38] reported the first synthesis of highly fluorescent DDT capped CIS/ZnS core/shell QDs using the solvothermal method. Indium acetate ($In(Ac)_3$), Cu(I) iodide (CuI) and DDT were used to synthesize the core CIS QDs in octadecene (ODE) at 180 °C for 5–6 h. Zinc acetate with potassium ethyl xanthogenate was used to form ZnS shell over the CIS core at 200 °C for 12 h. This produced yellow-to-red CIS/ZnS QDs with QY of 65 %. Jia et al., 2016 [41] synthesized CIS QDs via solvothermal approach by heating up a mixture of precursors i.e. zinc stearate ($ZnSt_2$), cuprous acetate ($Cu(OAc)_2$), indium acetate ($In(OAc)_3$) and oleylamine (OAm) in the presence of DDT/ODE. The PL intensity and peak position of the CIS and CIS/ZnS QDs were tuned by varying the excitation wavelength. This work emphasized the effect of excitation wavelength on the optical properties of CIS QDs. As the excitation wavelength increased from 550 nm to 630 nm, the PL peak position shifted from 665 to 685 nm. This shift in the PL peak position was attributed to the internal defect state of the material. Sugan et al., 2015 [42] synthesized AgInS using AgCl, In and S as reactants at 1:1:2 mole ratio respectively. Ethylenediamine was used as solvent and the synthesis performed at 200 °C for 8 h. PL emission peak of 620 nm where obtained with UV/VIS absorption at 590 nm. Differential thermal analysis (DTA) was used to determine the melting point of the AgInS and reported to be 956 °C.

2.1.3. Thermolysis

Thermolysis is a process by which nanoparticles are synthesized by heating metal complex precursors at high temperatures

Table 1
Overview of the experimental method of synthesizing CIS and CIS/ZnS QDs.

Material	Synthesis technique	Reference number
CIS	Hot-injection method	[37]
CIS, CIS/ZnS, AgInS	Solvothermal	[41,42,45,46]
CIS, CIS/ZnS	Thermolysis	[43,44]
CIS/ZnS	Non-injection	[47–49]
Cis, CIS/ZnS	Hydrothermal	[7,19,50]

together with a stabilizing compound. Choi et al. 2006 [43] reported the synthesis of CIS heterostructured nanocrystals via thermolysis of a mixture of Cu-oleate and In-oleate complexes in dodecane thiol. The shape of CIS nanocrystals could be varied from corn, bottle, to larva shapes by changing the reaction temperature and time. Lee et al., 2014 [44] described for the first time the use of a hybrid flow reactor to synthesize CIS/ZnS via thermolysis. The core QDs (CIS) were thermally grown at 210 °C for 1 min using DDT/ODE. ZnS was used to passivate the core at 320 °C for 2 mins. With ZnS shell growth, improved PL quantum yields (QY) of 60 % from initial values of 20 % was obtained. Thermolysis is advantageous as a fast-synthetic method for CIS QDs. The major disadvantage of this method is the presence of multiple peaks in the PL spectra even at wavelengths shorter than 700 nm.

2.1.4. Heating-up method

The heating-up method also known as the "non-injection" method involves the addition of reagents in one-pot and rapidly heating to the critical temperature for nucleation to occur. Thuy et al., 2014 [47] synthesized CIS/ZnS core/shell QDs by heating-up the copper (I) iodide (CuI), DDT, $In(Ac)_3$, zinc stearate and oleic acid as precursors at fast heating rate of 150–200 °C/min with diesel as reaction solvent. The highest quality of $CuInS_2$ QDs were obtained at reaction temperature of 210 °C for 15 min with the Cu:In molar ratio of 1:1. For large-scale synthesis, the heat-up method is considered the best method of choice [51]. Table 1 shows overview of the experimental method of synthesizing CIS and CIS/ZnS QDs.

2.2. Surface modifications

After the organic based synthesis, the fate of the QDs is often determined by the desired application. Although organic synthesis produces high quality QDs with good quantum yields, the hydrophobic nature of the synthesized QDs makes them unsuitable for some applications. For example, biological application of QDs which requires water-soluble materials [52]. Selection of stabilizing agents is thus very crucial in QDs synthesis. Stabilizing agents contribute to the surface functionalization, stability and solubility, all of which have significant impact on the optical properties and biocompatibility of the QDs. Furthermore, the selection of the ligand greatly determines the dispersive nature of the quantum dots in solution [27].

The basic principle for the metamorphosis of the hydrophobic quantum dots to water soluble biocompatible QDs is the conversion of the surface ligands. Many techniques have been reported for the conversion of hydrophobic QDs to hydrophilic biocompatible dots. These methods include the use of silica shell coating [53], ligand exchange [54] and amphiphilic polymer coating [55]. Fig. 2 depicts surface coating strategies (ligand exchange and amphiphilic strategies) for QDs (right side) and bioconjugation (left) of QDs using different biomolecules [27]. Other strategies not depicted in the diagram include the use of silica shell and encapsulation.

2.2.1. Ligand exchange

Ligand exchange is one of the most widely used methods for the surface modification of quantum dots. In general, it involves the exchange of hydrophobic ligands with bifunctional hydrophilic ligands. These hydrophilic ligands improve water solubility and offer attachment sites for secondary biomolecules such as drugs, antibodies or proteins on the surface of QDs [22,56–58]. Draaisma et al., 2016 [54], carried out ligand exchanged on DDT capped CIS/ZnS QDs and evaluated their use as luminescence down-shifting additives in photo-voltaic cells. In their work, DDT ligand was exchanged with thiol functionalized oligomeric caprolactone (Oligo-CL) polymer. The oligo-CL ligand was introduced to improve the compatibility of the CIS QDs with polyesterurethane resin and reduce QDs aggregation in the polymer matrix. The ligand exchange was performed at high temperatures and high concentration of the Oligo-CL was used to drive the equilibrium in favour of the exchange (as per Le Chantlier's principle). However, it is worth noting that excessive ligand to metal concentration can distort the QDs surface thereby decreasing the fluorescence intensity [59]. Gugula et al., 2016 [48] synthesized CIS and CIS/ZnS QDs in one-pot by non-injection method followed by surface modification. They functionalized the oleic acid (OA) capped CIS/ZnS QDs with MPA, MUD (11-mercapto-1-undecanol), and oleylamine (OAm) terminal ligands to make them suitable for LED application.

2.2.2. Encapsulation

Encapsulation approach often includes coating with amphiphilic molecules that contain functional groups such as $-NH_2$, –COOH, –SH or silica, polyethylene glycol (PEG) etc. [60]. The hydrophobic terminal of the amphiphilic ligand encapsulates the hydrophobic capped QDs whereas, the hydrophilic terminal end enables the dispersion of QDs in aqueous solution [61]. The encapsulation method is frequently used because it addresses the problems of poor luminescence quantum yields, aggregation and precipitation during surface modification. Booth et al., 2012 [49] performed encapsulation of DDT capped CIS/ZnS QDs on a commercial amphipol (amphiphilic polymers) poly (maleic anhydride-alt-1-tetradecene), 3-(dimethylamino)-1-propylamine derivative (PMAL-d). Amphipol encapsulation involved vigorous stirring of the CIS/ZnS–DDT coated QD with PMAL-d under argon flow at room temperature. The hydrodynamic diameter of the material was found to be to 13.7 ± 3.2 as determined by DLS.

2.3. Aqueous synthesis

Although the ligand exchange method allows customization of the CIS QDs to make them water soluble, it can lead to surface defects, which can affect the optical properties of the QDs and may alter the size of the QDs [21]. Hence the need for direct aqueous synthetic methods. Aqueous synthesis is reagent effective and less toxic. It also improves quantum dots water solubility and biocompatibility. Aqueous synthesis of quantum dots frequently encompasses the use of water-soluble thiols as capping agents. These thiol ligands are known for their high efficiency, extraordinary affinity and abundance [20,30]. In addition, they also allow the use of the QDs in biological applications without the need for further modification [60]. Typical aqueous synthesis involves the addition of the precursors at room temperature in the presence of stabilizing agents such as thiol groups (MPA, GSH, TGA) followed by heating under reflux [19,62]. Aqueous synthesis of CIS quantum dots is still in its infancy and thus much work is still required to perfect the reaction conditions.

Zhang et al., 2015 reported the synthesis of water soluble CIS and ZCIS QDs at pH 9 using $InCl_3$, $CuCl_2$ as precursors and MPA as capping agent. They varied the feed ratio of Cu : In from 0.07 to 1.33 while the amount of MPA was set at the moles of 20Cu + 8In

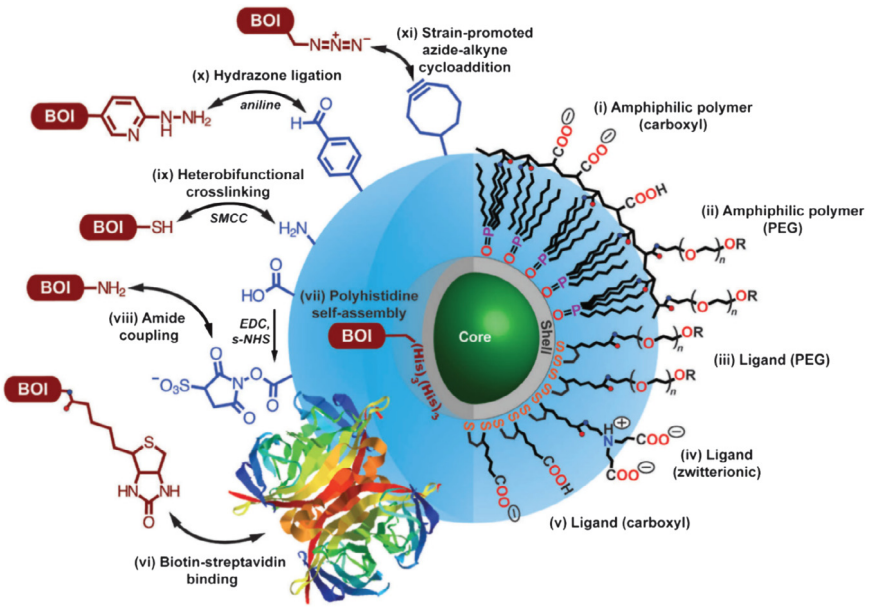

Fig. 2. Overview of different surface coating strategies (right side) and bioconjugation (left side) for QDs. Wegner et al., 2015 [27].

to obtain NIR QDs. The incorporation of Zn into CIS QDs was used as a strategy to enhance the PL intensity, narrow down the emission spectral width and increase the ability to tune the emission wavelength of the nanoparticles. Chen et al., 2014 [19], used copper chloride and indium chloride precursors with dual stabilizers (TGA and sodium citrate) to synthesis CIS/ZnS core/shell QDs by using a pressure cooker for large scale production. Approximately 3 grams of CIS/ZnS QDs were produced. The emission wavelengths can be varied from 545 to 610 nm by tuning Cu: In molar ratio and an addition of three ZnS monolayers. They maximum QY obtained was 40%. Lack of comparable results in the optical properties and crystal structures of CIS or zinc copper indium sulphide (ZCIS) QDs suggests that there are complexities and uncertainties in making their respective multi-ternary nanocrystals [63]. Wang et al., 2017 [50] synthesized AgInS using electric pressure cooker. Polyethyleneimine (PEI) was used as ligand. PLQY of 32% were obtained with UV/VIS absorption edge of AIS QDs at 460 nm. The PL spectrum consisted of a strong broad band ranging from 300 to 550 nm with a maximum at 420 nm. The AIS QDs were used as H_2O_2 sensors via electron-transfer quenching. The fluorescence of the QDs was used to quantify for glucose via the conversion of glucose into gluconic acid and H_2O_2 under catalyzation of glucose oxidase.

2.4. Effect of synthetic parameters

QDs can be tailored to required shape and size by varying different synthetic parameters such as capping ligand, precursor ratio, reaction time, temperature and pH [32,64,65]. It is worth noting here that, the optical and structural properties of QDs depend on their shape and size. The following section will look at the effect of these parameters on the properties of CIS QDs.

2.4.1. Precursor ratio

PL peak position and intensity of the CIS QDs can be optimized by varying the Cu:In ratio. Jia et al., 2017 [66], synthesized CIS/ZnS QDs using different Cu: In ratio from 1:2 to 1: 48 and studied their effects on optical properties. As the Cu: In ratio decreased, a shift to shorter wavelengths was observed indicating the widening of the band gap under poor-Cu conditions (Fig. 3). Zheng et al., 2016 [67] synthesized CIS/ZnS QDs with 20% photoluminescence quantum yield (PLQY) at gram-scale. They examined different molar ratios of Cu: In and found that, Cu-deficient CIS QDs produced higher PLQY. Kim et al., 2017 [32] synthesized NIR CIS QDs and were able to tune the PL peak position from 680 nm to 850 nm by tuning the Cu: In ratio from 0.25:1 to 2:1. Typically, the red-NIR emission is attributed to the donor–acceptor pair (DAP) transition, where In_{Cu} (In substituted at the Cu site) and/or V_S (S vacancy) probably act as donor states with V_{Cu} (Cu vacancy) as an acceptor state. For CuInS QD, Cu plays an important role in determining the emission peak with the mobility of Cu and its migration towards surface layers often resulting in non-uniform composition distribution [68–70]. Whereas for AgInS, the most sensitive chemical precursors are In and S. Variations in Ag ratio showed no effect on optical properties when Liu et al., 2013 [70] synthesized AgInS using oleylamine-sulphur solution, silver nitrate and indium acetate as precursor sources.

2.4.2. Reaction temperature and time

Theoretically, increasing the reaction temperature and time makes reaction precursors more reactive, which is beneficial for nanocrystals growth. However, prolonged reaction times may lead to induced aggregation of small crystals with broad size distribution and affects stability of the QDs. For organometallic synthesis, high temperatures and long reaction times often result in the precipitation of the QDs [71]. During the core (CIS) synthesis, increasing the reaction time generally shifts the PL spectra to longer wavelength due to particle growth, whereas in the shell growth (ZnS), the spectra will be blue shifted due to the extent of Zn ion diffusion into the core CIS as previously discussed. Kim et al., 2017 [32] synthesized NIR emitting DDT capped CIS/ZnS QDs in ODE by tuning the temperature from 180 °C to 250 °C during ZnS shell growth to control the Zn ion diffusion. At lower temperatures, they reported lower diffusion rates than that at higher temperature because the activation energy for diffusion was affected by temperature. A few studies have been reported on the direct aqueous synthesis of CIS and CIS/ZnS QDs where low temperatures (90–95 °C) have been used [7,20,72]. It has also been reported that the CIS crystal structure can be varied by changing the reaction temperatures [21].

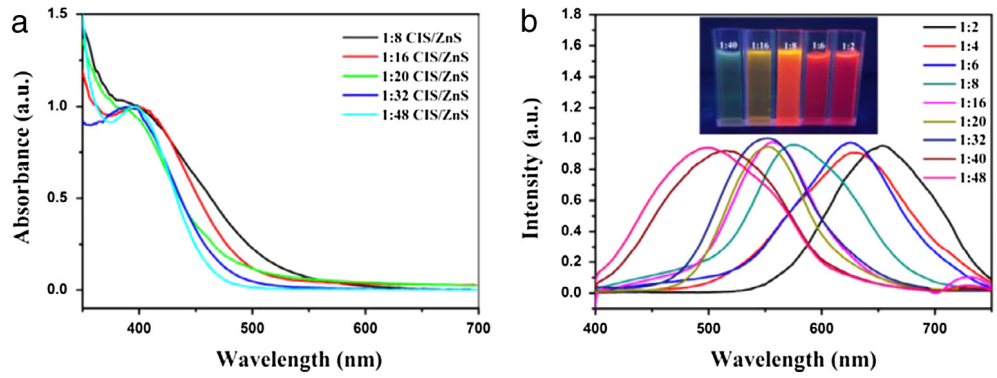

Fig. 3. The UV–Vis absorption spectra (a) and PL spectra (b) of CIS/ZnS core/shell QDs with different Cu:In ratios. *Inset:* Corresponding fluorescent images (Jia et al., 2017) [66].

2.4.3. pH

In the aqueous synthesis of CIS QDs, the reaction pH play an important role in the optical properties. Xiong et al., 2013 [46] investigated the effect of pH on the photoluminescence of glutathione capped CIS/ZnS NCs. Higher PL intensities was obtained at pH 8 among the other pH investigated (pH = 3–11). Chen et al., 2013 [20] studied the synthesis of CIS QDs using dual stabilizers glutathione and sodium citrate at pH 5.5 using Cu:In of 0.25 (1:4). Their result showed increased PL intensities and higher PLQY under weak acidic medium. Furthermore, at basic medium, the CIS core tend to aggregate with low PLQY due to probable formation of indium hydroxide.

3. Conjugation of QDs

Numerous strategies have been employed to conjugate the QDs to biomolecules. Conjugation is commonly reported as the covalent coupling of molecules on the surface of QDs as it forms stable linkages using cross-linker molecules [73]. Non-covalent conjugation techniques include; electrostatic attachment, encapsulation and adsorption of the material on the nanoparticle surface. The selection of the conjugation approach is based on QDs physicochemical properties such as chemical composition, availability of surface ligands and functional groups, size and inherent nanoparticle material [74]. Different binding affinities enable the conjugation of QDs to various functional biomolecules. These include the use of bio-functional ligands like MPA to link QDs to biomolecules (i.e. nucleic acids genes, oligomers, aptamers, and ribozymes/DNAzymes, proteins, peptides) [75]. Based on the above, various methods are available for bio-conjugation (Fig. 2). These include; biotin-streptavidin binding, heterobifunctional crosslinking, hydrazone ligation, strain-promoted azide-alkyne cycloaddition and 1-ethyl-3-(3-dimethylaminopropyl) carbodiimide hydrochloride (EDC) N-Hydroxysuccinimide (NHS) EDC/NHS amide coupling [76–78].

In addition to EDC, different coupling reagents (*N,N'*-Dicycloh exylcarbodiimide (DCC), N,N'-diisopropylcarbodiimide (DIC), phosphonium) have also been investigated for conjugation [79,80]. It is, however, important to appreciate that coupling reagents are not applicable for all conjugation. Therefore, selection of reagents is crucial and very much dependent on the ligands, and/or the surface coating on the QDs. Feng et al., 2016 [18], used the EDC/NHS coupling for the conjugation of different colour emitting CIS/ZnS QDs (635–730 nm) to 5-aminolevulinic acid (ALA) (Fig. 4). The optical properties and the Förster resonance energy transfer (FRET) mechanism of the conjugates was also studied. Their result showed that after conjugation, the CIS/ZnS QD emitting at 635 nm experienced no shift however, the QDs at 660 and 730 nm exhibited a blue-shift of approximately 6 nm. Furthermore, a decrease in fluorescence lifetime after the conjugation due to FRET was also observed. This highlights the importance of conjugation as it enables the use of photosensitizers like ALA in PDT, which on their own, would not reach longer emission wavelengths for deeper tissue penetration. Furthermore, conjugation of QDs with specific ligands has enabled targeted molecular imaging. Liu et al., 2015 [81] coated CIS/ZnS QDs with an amphillic bioconjugate composed of bovine serum albumin (BSA) - poly(ε-caprolactone) (PCL) for targeted cell imaging. The CIS/ZnS QD- BSA/PCL conjugate showed good stability in PBS buffer, pH 7.4.

4. Cytotoxicity

Several factors including composition, size, charge and capping ligands influence the toxicity of nanoparticles. Among them, the composition of the QDs is the ballpark for evaluating its toxicity. However, one needs to take into consideration that no two QDs are alike and as their physicochemical properties differ, so does their toxicity levels [82]. II–VI or IV–VI QDs, which are made of toxic metal (Cd, Pb) have raised toxicity concerns. The major concern of these QDs is their potential to leak into surrounding environment especially once degraded. This, however, has not been reported with CIS QDs thus far. On the contrary several studies have reported high cell viability [49,83] for both bio-conjugated [18,59] and non-conjugated [11,19] CIS based QDs. Chen et al., 2014 [19] used human hepatoma (HepG2) cell line to evaluate the cytotoxicity of CIS/ZnS QDs using 3-(4,5-dimethylthiazol-2-y)-2,5-diphenyltetrazolium bromide (MTT) method. At concentrations of 0–40 μg/mL QDs, they observed low cytotoxicity making the material suitable for bioimaging application. In another development, Lv et al., 2016 [84] evaluated the cytotoxicity and in vitro phototherapy efficacy of the ZCIS QDs in the mouse mammary carcinoma cell line 4T1. At 200 μg/mL of QDs, the cell viability was almost 90%, which suggested that ZCIS QDs had very low cytotoxicity.

5. Characterization of quantum dots

Several techniques have been used to characterize the optical and structural properties of CIS QDs. CIS QDs in general are red emitting, and when coated with ZnS shell, they emit bright orange as shown in Fig. 5a. The main crystal structures of CIS QDs are hexagonal wurtzite, cubic zinc blende and tetragonal chalcopyrite that can be determined from their XRD patterns [11,85]. The shift in the CIS diffraction peak towards the ZnS crystal phase is often used as means of confirming the formation of ZnS layer on the CIS core (Fig. 5b) [86]. UV characterization of CIS QDs show band edges, which have been attributed to band gap transitions. CIS QDs

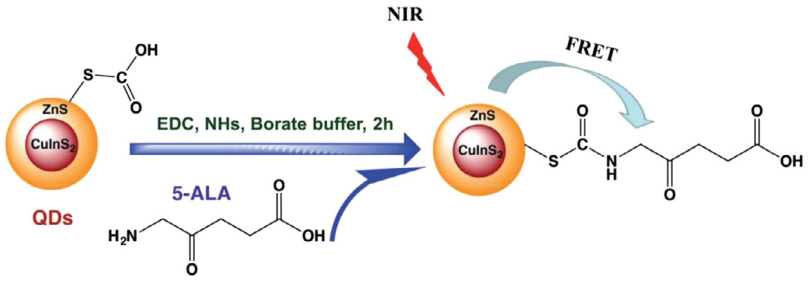

Fig. 4. Conjugation of CIS/ZnS to ALA using EDC/NHS via FRET mechanism. Feng et al., 2016 [18].

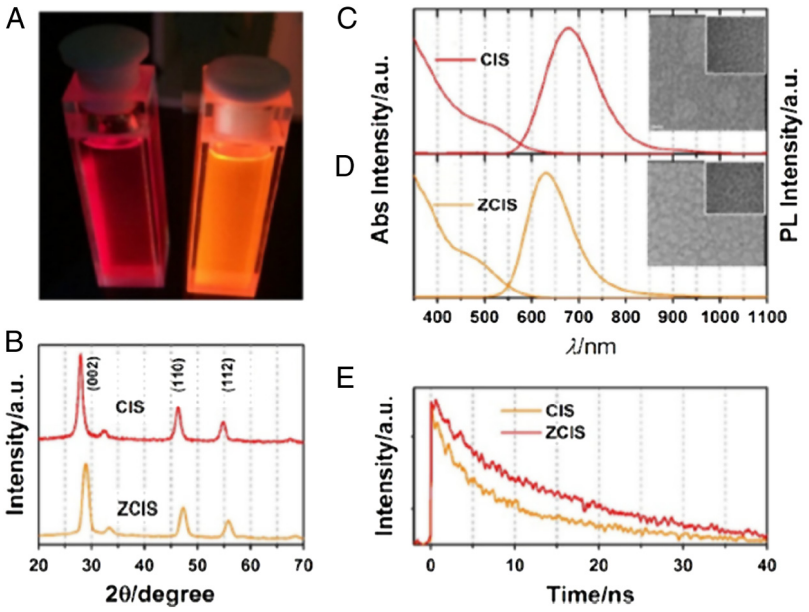

Fig. 5. (a) Digital photograph of naked CIS and core–shell structured CIS/ZnS from left to right. (b) XRD diagram of CIS QDs and ZCIS QDs. The absorption and emission spectra of CIS (c) and ZCIS (d) QDs in solution, (inset: the TEM image of #1, and #2 with different resolution of 50 nm (large one) and 5 nm (small one). (e) PL traces measured by TCSPC. Bi et al., 2016 [86]. For colloidal QDs, size distribution is affected by the growth of new nuclei during nucleation. Since size distribution is dependent on kinetic processes, control of synthetic parameters such as temperature is thus important in CIS QDs synthesis. CIS QDs size ranges from 2–3 nm for CIS, 3.8–8 nm for Zn(CIS) and 10 nm for Zn-CIS/ZnS [7,19,30,46]. Synthetic techniques such as the hot-injection, solvothermal and microwave irradiation have been used to produce material with narrow size distribution. (For interpretation of the references to colour in this figure legend, the reader is referred to the web version of this article.)

show no defined excitonic peaks (Fig. 5c and d). Alloying of CIS with Zn, or forming the ZnS shell over the CIS QDs generally shifts the spectra as already discussed. The absorption edge has been reported to be dependent on the CIS QD size [87], short-life and characteristic of the donor–acceptor (D–A) transition reported in I–III–VI nanocrystals [88].

Photoluminescence (PL) spectrum of CIS QDs often show multi-peaks with emissions at NIR regions. Several explanations have been given to explain this phenomenon [85]. Most studies have attributed the multi-peaks to surface defect [41,89] and nucleation events of CIS QDs [59]. Other reports attributed this to the existence of multi-phases (CuS, ZnS, Cu_2S) or inhomogeneous composition of the material [28,60]. Different synthetic methods and investigations (particularly in the understanding of their composition, optical and structural properties) are currently being done to prepare ternary CIS QDs with the prospect of getting a better understanding on the multi-peaks. Current developments on synthetic routes have addressed the multi-phases by optimizing parameters such as Cu:In ratio, temperature and pH [68,69]. Time-resolved PL (TRPL) spectra are often measured to understand the PL lifetimes in the recombination progress (Fig. 5e). Reported PL lifetimes for CIS ranges from 100 to 300 ns [90].

6. Applications

To date, significant work have been reported on CIS QDs applications in various industries such as medicine [6,16], electronics [7,8] and other technological industries [91]. Some of the applications of CIS based QDs are discussed below with particular focus on biological applications.

6.1. Bioimaging

Quantum dots sensitivity, stability, biocompatibility and minimal invasiveness make them ideal fluorescent probes for imaging techniques such as; optical imaging [92], magnetic resonance imaging [6,93], and nuclear imaging [94]. The CIS QDs have broad absorption, which make QDs to be excited to wavelengths close to their emission maximum. Their emission can be tuned to NIR wavelength suitable for *in-vivo* applications. For *in-vivo* applications, QDs must be less toxic, stable in biological media and hemocompatible [13,95]. It is important to note that biological medium is sensitive to many factors particularly size, shape, and the composition of nanoparticles. This makes the studying of the interaction of nanoparticles with biological environment essential. The hemocompatibility research using nanoparticles is therefore on-going with very few publications [13,96]. CIS QDs have shown

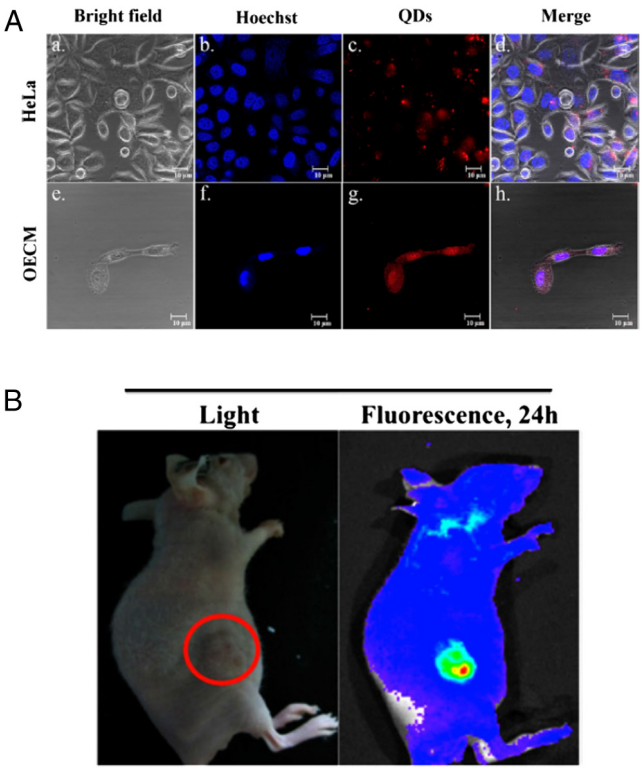

Fig. 6. (A) Confocal images of HeLa (a–d) and OECM (e–f) incubated with CIS/ZnS/OCMCS QDs for 12 h. Chen et al., 2015. (B) *In vivo* fluorescence images of a HeLa tumour-bearing mouse after intravenous injection of the CIS/ZnS–HSA–PEG–FA NCs in PBS. The area circled in red indicates the implanted tumour site. (Lee et al. 2014) [44]. (For interpretation of the references to colour in this figure legend, the reader is referred to the web version of this article.)

good stability in different media such as water, Dulbecco's modified eagle medium (DMEM), Foetal bovine serum (FBS) and Phosphate buffered saline (PBS) [59]. Helle et al., 2012 [97], studied the haemolytic capacity of PEGylated CIS/ZnS QDs encapsulated with lipid micelles. They compared the haemolytic capacity of CIS/ZnS QDs to CdTeSe/ZnS QDs. The study reported 80%–90% haemolysis with CdTeSe/ZnS QDs at 200 nM after 2 h of exposure. However, insignificant haemolysis was observed with CIS/ZnS QDs, which demonstrates the biocompatibility of the CIS QDs and displays its usefulness in *in-vivo* imaging applications.

Chen et al., 2015 [98], synthesized water-soluble O-carboxymethyl chitosan (OCMCS) coated CIS/ZnS QDs exhibiting cluster-like shape with size of 200 nm. The QDs are highly biocompatible to HeLa and OECM-1 cell lines with the cell viability of more than 90% as the concentration of QDs varied from 1 to 250 μg/mL. Using the confocal microscope, the localization of QDs in the cells with Hoechst as nucleus marker was also investigated (Fig. 6). The result showed that OCMCS-CIS/ZnS QDs entered into HeLa cells, and were localized in the nucleus. The same group, also successfully delivered CIS QDs to C. elegans which is a model organism in biology and studied their degradation. The oxidation state of CIS QDs was not changed after the treatment for 96 h, which validates the superior biocompatibility of the QDs.

Lee et al., 2014 [44] synthesized PEG coated CIS/ZnS QDs loaded with human serum albumin (HSA) and conjugated with folic acid (FA) to demonstrate the *in vivo* feasibility of CIS/ZnS bio-imaging system. The CIS/ZnS–HSA–PEG–FA QDs were injected in mice tail and efficiently directed towards the tumour and stayed in the tumour tissue. Tumour visualization was seen within few hours after intravenous injection of QDs and detected as faint spots in the tumour region with strong fluorescence intensity.

6.2. Biomedical applications

Photodynamic therapy is an emerging clinical trial in cancer therapy where photosensitizing (PS) drug is administrated to tumour followed by irradiation with light thereby producing reactive oxygen species to destroy the cancer cells. Quantum dots have been used in PDT to improve the optical properties of photosensitizing drugs. They are used as fluorescence resonance energy transfer (FRET) agents helping neighbouring conjugated photosensitizers under two-photon irradiation. NIR QDs like CIS QDs have two-photon absorptions in the first and second optical window of the tissue which has led to the treatment of deep-seated tumours using PDT [99,100]. Since these QDs can penetrate deeper, they experience minimal biological interferences from blood, melanin and haema pigments [75].

The loading of drugs in nanoparticles is one of the most investigated areas. QDs have been used in drug delivery systems due to their increased drug loading capacity, controlled release profile and improved therapeutic index of the drugs [101]. Many techniques have been used to load drugs to QDs which include adsorption, dispersion, and coupling [102]. Gao et al., 2014 [103] studied the drug delivery profile of PGA coated CIS QDs with doxorubicin (DOX) as a model anti-cancer drug. The QDs were able to deliver DOX to targeted cancer cells. Using the turn-on signal of CIS QDs, they monitored the DOX release *in-vitro* and could simultaneously use the QDs for imaging of the cancer cells. Drug delivery using QDs experiences some barriers which includes particle size and shape [104], surface charge [105], deformability and degradability. The understanding of these barriers and their effect is the current research focus on the use of QDs for drug delivery.

6.3. Other industrial applications

Applications of CIS are not limited to the above fields but expanding in all nanotechnology applications. CIS have been utilized for applications such as photovoltaic cells [54], white light emitting diodes [106] due to their large Stokes shift, high photoluminescence quantum yield (PLQY) and high absorption coefficient. Bai et al., 2016 [107], synthesized 6-mercaptohexanol (MCH) capped CIS QDs through ligand exchange and fabricated bright light emitting diode using these QDs as an emitting layer. The results showed that hydroxyl terminated ligand can tune the potential barriers and enhanced the electron injection efficiency between the layers. Chuang et al., 2014 [8] synthesized CIS/ZnS QDs with different Cu/In ratios for white light emitting diodes and obtained high colour rendering index values of 90. They further used these CIS/ZnS QDs as colour converters in combination with green light-emitting Ba_2SiO_4: Eu^{2+} phosphors and blue light-emitting diodes. Meinardi et al., 2015 [108] used CISe/ZnS QDs as solar concentrators due to their large absorption cross-sections. Due to the suppressed re-absorption and high emission efficiencies of the quantum dots, they obtained only 3.2% optical power efficiency. $CuInSe_2$ are highly attractive for bottom cells in tandem devices, as their bandgap are an excellent match to some of the best performing hybrid perovskites. Uhl et al., 2016 [109] produced a molecular-ink route to deposit $Cu(In,Ga)(S,Se)_2$ absorber layers. Copper-thiourea-chloride complex and an indium–DMSO-chloride complex were used to control the oxidation states, loss of metals during processing and to tailor the final composition of the absorber. CuIn (S,Se) at 1,00 eV and 1,15 eV bandgaps produced 13.0% and 14.7 % conversion efficiency respectively. With bulk-bandgaps of 1.87 eV and 1.98 eV for tetragonal ad orthorhombic phases respectively. $AgInS_2$ have also shown to be promising materials for photovoltaic applications [110].

7. Challenges with CIS based QDs

Although the I–III–VI quantum dots have shown greater advantage compared to the traditional II-VI QDs, they are not without their own challenges, especially their ternary compositions. These include the narrow band gaps (1.45 eV for CIS QDs) of the bulk material, which cannot be fully influenced by quantum confinement effect. The band gap thus becomes adjustable only within certain limits even with the incorporation of ZnS shell. CIS QDs have shown limited shape, composition, and size control, due to their intricate equilibria in multiple reactions between cation and anion precursors that exhibit different reactivity's. Furthermore, due to the Cu-S bond being weaker than the In-S, substantial variations in stoichiometry between Cu^{+} and In^{3+} during synthesis results in off-stoichiometry and phase complexity that trigger structural defects [83,111]. To address the latter, a number of researchers have used two stabilizing agents [17,19]. This has been proved to be particularly useful in balancing the reactivities of Cu and In as CIS QDs are able to accommodate large off-stoichiometry by forming various structural defects, which makes it difficult to obtain pure phase CIS products [11]. Doping of CIS/ZnS QDs with transition elements to address some of these challenges and to improve the optical and electronic properties has been reported. Gd-doped CuInS/ZnS were reported by Chang et al., 2016 [93] to improve the magnetic properties of ternary QDs as well as CIS/ZnS QYs and their photo-stability. Whereas, Mn^{2+} doped CuInS/ZnS QDs have been reported to provide long-lived and well-resolved peaks [112].

8. Conclusion

The I–III–VI ternary quantum dots (QDs) have seen a burst in development recently due to their excellent properties such as tuneable emissions to near-infrared regions, large Stokes Shift and most importantly their relatively lower toxicity compared to conventional II–VI QDs. Though several organic synthetic methods have been reported for these materials with excellent optical properties however, their bio-application requires further steps such as surface modification, ligand exchange and so on to make them biocompatible. Unfortunately, the final product after these processing usually have inferior optical properties such as PLQY compared to the parent material before modification. Direct aqueous synthesis on the other hand, is more promising for bioapplications apart from the fact that, it is more economically viable for industrial commercialization. However, these still face many challenges such as multiple PL peaks, blue shifting of the emission position after passivation and effect of cation and anion precursor reactivity. All these needs to be addressed by researchers in order to obtain product with similar or superior properties when compared to those obtained via organic synthesis. Furthermore, the mechanism behind the photoluminescence properties of these materials still need thorough investigation for proper understanding especially now that they are replacing the conventional Cd and Pb based QDs for bio applications. Nonetheless, the development of NIR ternary QDs especially CIS and CIS/ZnS quantum dots has brought a new dawn in the application of QDs particularly their biological applications for imaging, drug delivery and therapeutic processes.

Acknowledgements

The authors will like to thank National Research Foundation (NRF), South Africa under the Nanotechnology Flagship Programme (Grant no: 97983) and Thuthuka (Grant no: 107295) for financial support. The authors also thank Cape-Peninsula University, under the Teaching Development Grant for the study leave granted to NT.

References

[1] G.P.C. Drummen, Quantum dots - From synthesis to applications in biomedicine and life sciences, Int. J. Mol. Sci. 11 (2010) 154–163. http://dx.doi.org/10.3390/ijms11010154.
[2] J. Chomoucká, J. Drbohlavová, V. Adarrr, R. Kizek, J. Hubálek, Synthesis of glutathione-coated Quantum Dots, in: ISSE 2009 32nd Int. Spring Semin. Electron. Technol. Hetero Syst. Integr. Path to New Solut. Mod. Electron. - Conf. Proc. 2009. pp. 1–19. http://doi.org/10.1109/ISSE.2009.5206958.
[3] M.A. Walling, J.A. Novak, J.R.E. Shepard, Quantum dots for live cell and in vivo imaging, Int. J. Mol. Sci. 10 (2009) 441–491. http://dx.doi.org/10.3390/ijms10020441.
[4] O.S. Oluwafemi, V. Ncapayi, O. Olubomehin, O.A. Osibote, S.P. Songca, Materials science in semiconductor processing A facile non-organometallic synthesis of hexadecylamine-capped ZnSe nanoparticles, Mater. Sci Semicond. Proc. 27 (2014) 427–432. http://dx.doi.org/10.1016/j.mssp.2014.07.007.
[5] S.O. Oluwafemi, N. Revaprasadu, A.J. Ramirez, A novel one-pot route for the synthesis of water-soluble cadmium selenide nanoparticles, J. Cryst. Growth 310 (2008) 3230–3234. http://dx.doi.org/10.1016/j.jcrysgro.2008.03.032.
[6] J. Zhou, Y. Yang, C.Y. Zhang, Toward biocompatible semiconductor quantum dots: From Biosynthesis and bioconjugation to biomedical application, Chem. Rev. 115 (2015) 11669–11717. http://dx.doi.org/10.1021/acs.chemrev.5b00049.
[7] X. Kang, Y. Yang, L. Huang, Y. Tao, L. Wang, D. Pan, Large-scale synthesis of water-soluble CuInSe2/ZnS and AgInSe2/ZnS core/shell quantum dots, Green Chem. 17 (2015) 4482–4488. http://dx.doi.org/10.1039/C5GC00908A.
[8] C.-H.M. Chuang, P.R. Brown, V. Bulović, M.G. Bawendi, Improved performance and stability in quantum dot solar cells through band alignment engineering, Nature Mater. 13 (2014) 796–801. http://dx.doi.org/10.1038/nmat3984.
[9] C. Li, W. Chen, D. Wu, D. Quan, Z. Zhou, J. Hao, J. Qin, Large stokes shift and high efficiency luminescent solar concentrator incorporated with CuInS 2 / ZnS quantum dots, Nat. Publ. Gr. (2015) 1–9. http://dx.doi.org/10.1038/srep17777.
[10] D.C. Gary, M.W. Terban, S.J.L. Billinge, B.M. Cossairt, Two-step nucleation and growth of InP quantum dots via magic-sized cluster intermediates, Chem. Mater. 27 (2015) 1432–1441. http://dx.doi.org/10.1021/acs.chemmater.5b00286.33.
[11] B. Zhang, Y. Wang, C. Yang, S. Hu, Y. Gao, Y. Zhang, Y. Wang, H.V. Demir, L. Liu, K.-T. Yong, The composition effect on the optical properties of aqueous synthesized Cu–In–S and Zn–Cu–In–S quantum dot nanocrystals, Phys. Chem. Chem. Phys. 17 (2015) 25133–25141. http://dx.doi.org/10.1039/C5CP03312H.
[12] P. Chuang, C.C. Lin, R. Liu, Emission-tunable CuInS 2 / ZnS quantum dots: structure, optical properties, and application in white light-emitting diodes with high color rendering index, ACS Appl. Mater. Interfaces, 6 (2014) 15379–15387. http://dx.doi.org/10.1021/am503889z.
[13] E.S. Speranskaya, C. Sevrin, S. De Saeger, Z. Hens, I.Y. Goryacheva, C. Grandfils, Synthesis of hydrophilic CuInS2/ZnS quantum dots with different polymeric shells and study of their cytotoxicity and hemocompatibility, ACS Appl. Mater. Interfaces 8 (2016) 7613–7622. http://dx.doi.org/10.1021/acsami.5b11258.
[14] K.E. Knowles, K.H. Hartstein, T.B. Kilburn, A. Marchioro, H.D. Nelson, P.J. Whitham, D.R. Gamelin, Luminescent colloidal semiconductor nanocrystals containing copper: Synthesis, photophysics, and applications, Chem. Rev. (2016). http://dx.doi.org/10.1021/acs.chemrev.6b00048. acs.chemrev.6b00048.
[15] Q.A. Akkerman, A. Genovese, C. George, M. Prato, I. Moreels, A. Casu, S. Marras, A. Curcio, A. Scarpellini, T. Pellegrino, L. Manna, V. Lesnyak, From binary Cu 2 S to ternary Cu-In-S and quaternary Cu-In-Zn-S nanocrystals with tunable composition via partial cation exchange, ACS Nano (2015) 521–531. http://dx.doi.org/10.1021/nn505786d.
[16] G. Lv, W. Guo, W. Zhang, T. Zhang, S. Li, S. Chen, Near-Infrared Emission CuInS/ZnS Quantum Dots: All-in-One Theranostic Nanomedicines with Intrinsic Fluorescence/Photoacoustic Imaging for Tumor Phototherapy, 2016. http://dx.doi.org/10.1021/acsnano.6b05419.
[17] T. Jiang, J. Song, H. Wang, X. Ye, H. Wang, Aqueous synthesis of color tunable Cu doped Zn-In-S/ZnS nanoparticles in the whole visible region for cellular imaging In: Zn, J. Mater. Chem. B 3 (2015) 2402–2410. http://dx.doi.10.1039/C4TB01957A.
[18] Y. Feng, L. Liu, S. Hu, Y. Liu, Y. Ren, X. Zhang, Forster resonance energy transfer properties of a new type of near-infrared excitation PDT photosensitizer: CuInS 2 /ZnS quantum dots-5-aminolevulinic acid conjugates, RSC Adv. 6 (2016) 55568–55576. http://dx.doi:10.1039/C6RA06937A.
[19] Y. Chen, S. Li, L. Huang, D. Pan, Low-cost and gram-scale synthesis of water-soluble Cu-In-S/ZnS core/shell quantum dots in an electric pressure cooker, Nanoscale 6 (2014) 1295–1298. http://doi:10.1039/c3nr05014a.
[20] Y. Chen, S. Li, L. Huang, D. Pan, Green and facile synthesis of water-soluble Cu — In — S/ZnS core/shell quantum dots, Inorg. Chem. 52 (2013) 12–14. http://dx.doi.org/10.1021/ic400083w.

[21] A.D.P. Leach, J.E. Macdonald, Optoelectronic properties of CuInS 2 nanocrystals and their origin, J. Phys. Chem. Lett. 7 (2016) 572–583. http://dx.doi.org/10.1021/acs.jpclett.5b02211.

[22] A.S. Karakoti, R. Shukla, R. Shanker, S. Singh, Surface functionalization of quantum dots for biological applications, Adv. Colloid Interface Sci. 215 (2015) 28–45. http://dx.doi.org/10.1016/j.cis.2014.11.004.

[23] V. Kocevski, J. Rusz, O. Eriksson, D.D. Sarma, First-principles study of the influence of different interfaces and core types on the properties of CdSe / CdS core–shell nanocrystals, Nat. Publ. Gr., 2015, pp. 1–12. http://dx.doi.org/10.1038/srep10865.

[24] L. Yu, H. Ruan, Y. Zheng, D. Li, A facile solvothermal method to produce ZnS quantum dots-decorated graphene nanosheets with superior photoactivity, Nanotechnology 24 (2013) 375601. http://dx.doi.org/10.1088/0957-4484/24/37/375601.

[25] U. Baishya, D. Sarkar, ZnS nanocomposite formation: Effect of ZnS source concentration ratio, Indian J. Pure Appl. Math. 49 (2011) 186–189.

[26] W. Guo, N. chen, Y. Tu, C. Dong, B. Zhang, C. Hu, J. Chang, Synthesis of Zn-Cu-In-S/ZnS Core/Shell quantum dots with inhibited blue-shift photoluminescence and applications for tumor targeted bioimaging, Theranostics 3 (2013) 99–108. http://dx.doi.org/10.7150/thno.5361.

[27] K.D. Wegner, N. Hildebrandt, N. Hildebrandt, Chem Soc Rev Quantum dots: bright and versatile in vitro and in vivo fluorescence imaging biosensors, Chem. Soc. Rev. 44 (2015) 4792–4834. http://dx.doi.org/10.1039/C4CS00532E.

[28] L. Li, T.J. Daou, I. Texier, T.T. Kim Chi, N.Q. Liem, P. Reiss, Highly luminescent CuInS 2 /ZnS core/shell nanocrystals: cadmium-free quantum dots for in vivo imaging, Chem. Mater. 21 (2009) 2422–2429. http://dx.doi.org/10.1021/cm900103b.

[29] C. Wada, Y. Iso, H. Sasaki, Preparation and photoluminescence properties of yellow-emitting CuInS2/ZnS quantum dots embedded in TMAS-derived silica, RSC Adv. 7 (2017) 7936–7943. http://dx.doi.org/10.1039/C7RA00081B.

[30] A. Zhang, C. Dong, L. Li, J. Yin, H. Liu, X. Huang, J. Ren, Non-blinking (Zn)CuInS/ZnS quantum dots prepared by in situ interfacial alloying approach, Sci. Rep. 5 (2015) 15227. http://dx.doi.org/10.1038/srep15227.

[31] M. Fu, W. Luan, S. Tu, L. Mleczko, Green synthesis of CuInS 2 / ZnS nanocrystals with high photoluminescence and stability, J. Nanomat. (2015) 842365.

[32] Y. su Kim, Y. Lee, Y. Kim, D. Kim, H.S. Choi, J.C. Park, Y.S. Nam, D.Y. Jeon, Synthesis of efficient near-infrared-emitting $CuInS_2$ /ZnS quantum dots by inhibiting cation-exchange for bio application, RSC Adv. 7 (2017) 10675–10682. http://dx.doi.org/10.1039/C6RA27045J.

[33] A. Zhang, C. Dong, L. Li, J. Yin, H. Liu, X. Huang, J. Ren, Non-blinking (Zn)CuInS/ZnS quantum dots prepared by in situ interfacial alloying approach, Sci. Rep. 5 (2015) 15227. http://dx.doi.org/10.1038/srep15227.

[34] X. Wang, Z. Liang, X. Xu, N. Wang, J. Fang, J. Wang, G. Xu, A high efficient photoluminescence Zn-Cu-In-S/ZnS quantum dots with long lifetime, J. Alloys Compd. 640 (2015) 134–140. http://dx.doi.org/10.1016/j.jallcom.2015.03.249.

[35] J. Du, Z. Du, J. Hu, Z. Pan, Q. Shen, J. Sun, D. Long, H. Dong, L. Sun, X. Zhong, L. Wan, Zn — Cu — In — Se quantum dot solar cells with a certified power conversion efficiency of 11.6%, J. Am. Chem. Soc. 138 (2016) 4201–4209. http://dx.doi.org/10.1021/jacs.6b00615.

[36] P. Reiss, M. Carrie, C. Lincheneau, L. Vaure, S. Tamang, Synthesis of Semiconductor Nanocrystals. Focusing on Nontoxic and Earth-Abundant Materials, 2016. http://dx.doi.org/10.1021/acs.chemrev.6b00116.

[37] Y. Vahidshad, R. Ghasemzadeh, A. Irajizad, S.M. Mirkazemi, C. Solvent, Synthesis and Characterization of Copper Indium Sulfide Chalcopyrite Structure with Hot Injection Method, 3, 2013, 145–154.

[38] Y. Yuan, F. Riehle, H. Gu, R. Thomann, G. Urban, M. Krüger, Critical parameters for the scale-up synthesis of quantum dots, J. Nanosci. Nanotechnol. 10 (2010) 6041–6045. http://dx.doi.org/10.1166/jnn.2010.2564.

[39] J. Hua, H. Cheng, X. Yuan, Y. Zhang, M. Liu, X. Meng, RSC Advances Photoluminescence quenching and electron transfer in CuInS 2 / ZnS core / shell quantum dot and, RSC Adv. 5 (2015) 30981–30988. http://dx.doi.org/10.1039/C5RA04542H.

[40] G. Demazeau, Solvothermal reactions: an original route for the synthesis of novel materials. J. Mat. Sci. 43 (2008) 2104–2114. http://dx.doi:10.1007/s10853-007-2024-9.

[41] Y. Jia, H. Wang, Z. Yan, L. Deng, H. Dong, RSC Advances A facile method for the synthesis of CuInS 2–ZnS quantum dots with tunable photoluminescent, RSC Adv. 6 (2016) 93303–93308. http://dx.doi.org/10.1039/C6RA14733J.

[42] S. Sugan, R. Dhanasekaran, Synthesis of AgInS2 semiconductor nano crystals by solvothermal method, Mater. Sci. Eng. 73 (2015) 012147. http://dx.doi.org/10.1088/1757-899X/73/1/012147.

[43] S.H. Choi, E.G. Kim, T. Hyeon, One-pot synthesis of copper-indium sulfide nanocrystal heterostructures with acorn, bottle, and larva shapes, J. Am. Chem. Soc. 128 (2006) 2520–2521. http://dx.doi.org/10.1021/ja0577342.

[44] J. Lee, C.-S. Han, Large-scale synthesis of highly emissive and photostable CuInS2/ZnS nanocrystals through hybrid flow reactor, Nanoscale Res. Lett. 9 (2014) 78. http://dx.doi.org/10.1186/1556-276X-9-78.

[45] D. Nam, W. Song, H. Yang, Facile, air-insensitive solvothermal synthesis of emission-tunable CuInS2/ZnS, J. Mater. Chem. (2011) 18220–18226. http://dx.doi.org/10.1039/C1JM12437D.

[46] W. Xiong, G. Yang, X. Wu, J. Zhu, Aqueous Synthesis of Color-Tunable CuInS 2 /ZnS Nanocrystals for the Detection of Human Interleukin 6, 2013.

[47] N. Thi, M. Thuy, T. Thi, K. Chi, U. Thi, D. Thuy, N. Quang, Low-cost and large-scale synthesis of CuInS 2 and CuInS 2/ZnS quantum dots in diesel, Opt. Mat. 37 (2014) 823–827. http://dx.doi.org/10.1016/j.optmat.2014.09.016.

[48] K. Gugula, L. Stegemann, P.J. Cywiński, C.A. Strassert, M. Bredol, Facile surface engineering of $CuInS_2$ /ZnS quantum dots for LED down-converters, RSC Adv. 6 (2016) 10086–10093. http://dx.doi.org/10.1039/C5RA26331J.

[49] M. Booth, A.P. Brown, S.D. Evans, K. Critchley, Determining the concentration of CuInS 2 quantum dots from the size-dependent molar extinction coefficient, Chem. Mater. 24 (2012) 2064–2070. http://dx.doi.org/10.1021/cm300227b.

[50] L. Wang, X. Kang, D. Pan, Gram-scale synthesis of hydrophilic PEI-coated AgInS 2 quantum dots and its spplication in hydrogen peroxide/glucose detection and cell imaging, Inorg. Chem. 56 (2017) 6122–6130. http://dx.doi.org/10.1021/acs.inorgchem.7b00053.

[51] J. Park, S.-W. Kim, CuInS2/ZnS core/shell quantum dots by cation exchange and their blue-shifted photoluminescence, J. Mater. Chem. 21 (2011) 3745. http://dx.doi.org/10.1039/c0jm03194a.

[52] H. Chen, T. Wang, K. Li, Q. He, X. Hou, R. Yang, B. Wang, Journal of Colloid and Interface Science Effects of surface modification of quantum dots on viability and migration of triple-negative breast cancer cells, J. Colloid Interface Sci. 485 (2017) 51–58. http://dx.doi.org/10.1016/j.jcis.2016.09.024.

[53] N.O. Farrell, Silicon nanoparticles: applications in cell biology and medicine, Inter. J. Nanomedicine 4 (2006) 451-472.

[54] G.J.J. Draaisma, D. Reardon, A.P.H.J. Schenning, S.C.J. Meskers, , C.W.M. Bastiaansen, Ligand exchange as a tool to improve quantum dot miscibility in polymer composite layers used as luminescent down-shifting layers for photovoltaic applications, J. Mater. Chem. C 4 (2016) 5747–5754. http://dx.doi.org/10.1039/C6TC01261B.

[55] B. Yang, Y. Li, X. Sun, X. Meng, P. Chen, N. Liu, A pH-responsive drug release system based on doxorubicin conjugated amphiphilic polymer coated quantum dots for tumor cell targeting and tracking, J. Chem. Technol. Biotechnol. 88 (2013) 2169–2175. http://dx.doi.org/10.1002/jctb.4081.

[56] T. Jiang, J. Song, H. Wang, X. Ye, H. Wang, W. Zhang, M. Yang, R. Xia, L. Zhu, X. Xu, Aqueous synthesis of color tunable Cu doped Zn–In–S / ZnS nanoparticles in the whole visible region for cellular imaging †, J. Mater. Chem. B Mater. Biol. Med. 3 (2015) 2402–2410. http://dx.doi.org/10.1039/C4TB01957A.

[57] N.T.K. Thanh, L.A.W. Green, Functionalisation of nanoparticles for biomedical applications, Nano Today 5 (2010) 213–230. http://dx.doi.org/10.1016/j.nantod.2010.05.003.

[58] R. Dey, S. Mazumder, M.K. Mitra, S. Mukherjee, G.C. Das, Review: Biofunctionalized quantum dots in biology and medicine, J. Nanomater. 200 (2009) 9. http://dx.doi.org/10.1155/2009/815734.

[59] A. Arshad, R. Akram, S. Iqbal, F. Batool, B. Iqbal, Aqueous synthesis of tunable fluorescent, semiconductor CuInS 2 quantum dots for bioimaging, Arab. J. Chem. (2016) 4–11. http://dx.doi.org/10.1016/j.arabjc.2016.10.002.

[60] Y. Zhang, A. Clapp, Overview of stabilizing ligands for biocompatible quantum dot nanocrystals, Sensors 11 (2011) 11036–11055. http://dx.doi.org/10.3390/s111211036.

[61] G. Palui, F. Aldeek, W. Wang, H. Mattoussi, Strategies for interfacing inorganic nanocrystals with biological systems based on polymer-coating, Chem. Soc. Rev. 44 (2014) 193–227. http://dx.doi.org/10.1039/c4cs00124a.

[62] Y. Feng, L. Liu, S. Hu, Y. Liu, Y. Ren, X. Zhang, RSC Advances Fo¨rster resonance energy transfer properties of a new type of near-infrared excitation PDT, RSC Adv. 6 (2016) 55568–55576. http://dx.doi.org/10.1039/C6RA06937A.

[63] A. Zhang, C. Dong, L. Li, J. Yin, H. Liu, X. Huang, Non-blinking (Zn) CuInS / ZnS Quantum Dots Prepared by In Situ Interfacial Alloying Approach, Nat. Publ. Gr., 2015, pp. 1–13. http://dx.doi.org/10.1038/srep15227.

[64] Y. Xu, T. Chen, X. Hu, W. Jiang, L. Wang, W. Jiang, J. Liu, Journal of colloid and interface science the off-stoichiometry effect on the optical properties of water-soluble copper indium zinc sulfide quantum dots, J. Colloid Interface Sci. 496 (2017) 479–486. http://dx.doi.org/10.1016/j.jcis.2017.02.049.

[65] T. Akdas, M. Haderlein, J. Walter, B. Apeleo Zubiri, E. Spiecker, W. Peukert, Continuous synthesis of $CuInS_2$ quantum dots, RSC Adv. 7 (2017) 10057–10063. http://dx.doi.org/10.1039/C6RA27052B.

[66] L. Jia, Y. Wang, Q. Nie, B. Liu, E. Liu, X. Hu, J. Fan, Aqueous-synthesis of CuInS 2 core and CuInS 2/ZnS core/shell quantum dots and their optical properties, Mater. Lett. 200 (2017) 27–30. http://dx.doi.org/10.1016/j.matlet.2017.04.082.

[67] Y. Zheng, B. Sadeghimakki, N.M.S. Jahed, S. Sivoththaman, Scalable Non-injection synthesis of Cd-Free copper indium sulfide/zinc sulfide quantum dots for third-gen photovoltaic application, MRS Adv. 1 (2016) 2193–2198. http://dx.doi.org/10.1557/adv.2016.536.

[68] B. Xie, B. Hu, L. Jiang, G. Li, Z. Du, The phase transformation of CuInS 2 from chalcopyrite to wurtzite, Nanoscale Res. Lett. 10 (2015) 86. http://dx.doi.org/10.1186/s11671-015-0800-z.

[69] H. Chen, Y. Yeh, C. Hao, J. Zhi, C. Wang, Removal of CuS phases from electrodeposited CuInS 2 films, 40, 2014, 67–72. http://dx.doi.org/10.1016/j.ceramint.2013.05.104.
[70] L. Liu, R. Hu, W. Law, I. Roy, J. Zhu, L. Ye, S. Hu, Optimizing the synthesis of red- and near-infrared CuInS2 and AgInS2 semiconductor nanocrystals for bioimaging, Analyst 138 (2013) 6144–6153. http://dx.doi.org/10.1039/c3an01030a.
[71] S. Liu, H. Zhang, Y. Qiao, X. Su, One-pot synthesis of ternary CuInS2 quantum dots with near-infrared fluorescence in aqueous solution, RSC Adv. 2 (2012) 819. http://dx.doi.org/10.1039/c1ra00802a.
[72] A. Raevskaya, O. Rosovik, A. Kozytskiy, O. Stroyuk, V. Dzhagan, D.R.T. Zahn, Non-stoichiometric Cu–In–S/ZnS nanoparticles produced in aqueous solutions as light harvesters for liquid-junction photoelectrochemical solar cells, RSC Adv. 6 (2016) 100145–100157. http://dx.doi.org/10.1039/C6RA18313A.
[73] I.L. Medintz, H.T. Uyeda, E.R. Goldman, H. Mattoussi, Quantum dot bioconjugates for imaging, labelling and sensing, Nature Mater. 4 (2005) 435–446. http://dx.doi.org/10.1038/nmat1390.
[74] L.B. Kim, E. Sapsford, W. Russ Algar, Functionalizing nanoparticles with biological molecules: developing chemistries that facilitate nanotechnology, J. Am. Chem. Soc. 113 (2013) 1904–2074.
[75] S. Kamila, C. Mcewan, D. Costley, J. Atchison, Y. Sheng, G.R.C. Hamilton, C. Fowley, J.F. Callan, Diagnostic and therapeutic applications of quantum dots in nanomedicine, Top Curr. Chem. 370 (2016) 203–224. http://dx.doi.org/10.1007/978-3-319-22942-3_7.
[76] J. Zhang, G. Hao, C. Yao, S. Hu, C. Hu, B. Zhang, Paramagnetic albumin decorated $CuInS_2$ /ZnS QDs for $CD133^+$ glioma bimodal MR/fluorescence targeted imaging, J. Mater. Chem. B 4 (2016) 4110–4118. http://dx.doi.org/10.1039/C6TB00834H.
[77] R. Sperling, W.J. Parak, Surface modification, functionalization and bioconjugation of colloidal inorganic nanoparticles, Philos. Trans. R. Soc. 368 (2010) 1333–1383. http://dx.doi.org/10.1098/rsta.2009.0273.
[78] X. Gao, L. Yang, J.A. Petros, F.F. Marshall, J.W. Simons, S. Nie, In vivo molecular and cellular imaging with quantum dots, Curr. Opin. Biotechnol. 16 (2005) 63–72. http://dx.doi.org/10.1016/j.copbio.2004.11.003.
[79] V. Biju, Chemical modifications and bioconjugate reactions of nanomaterials for sensing, imaging, drug delivery and therapy, Chem. Soc. Rev. 43 (2014) 744–764. http://dx.doi.org/10.1039/C3CS60273G.
[80] K.-T. Yong, G. Xu, I. Roy, Engineering arginine cross-linked mercaptoundecanoic acid CdSe/CdS/ZnS quantum dots for two-photon imaging of live cancer cells, Chem. Commun. 47 (2011) 2901. http://dx.doi.org/10.1039/c0cc05041e.
[81] Z. Liu, N. Chen, C. Dong, W. Li, W. Guo, H. Wang, S. Wang, J. Tan, Y. Tu, J. Chang, Facile construction of near infrared fluorescence nanoprobe with amphiphilic protein-polymer bioconjugate for targeted cell imaging, ACS Appl. Mater. Interfaces 7 (2015) 18997–19005. http://dx.doi.org/10.1021/acsami.5b05406.
[82] R. Hardman, Review a toxicologic review of quantum dots: toxicity depends on physicochemical and environmental factors, Environ. Health Persp. 114 (2006) 165–172. http://dx.doi.org/10.1289/ehp.8284.
[83] S.S. Chetty, S. Praneetha, S. Basu, C. Sachidanandan, A.V. Murugan, Sustainable, rapid synthesis of bright-luminescent CuInS2-ZnS Alloyed Nanocrystals: Multistage nano-xenotoxicity assessment and intravital fluorescence bioimaging in Zebrafish-Embryos, Sci. Rep. 6 (2016) 26078. http://dx.doi.org/10.1038/srep26078.
[84] G. Lv, W. Guo, W. Zhang, T. Zhang, S. Li, S. Chen, Near-infrared emission CuInS/ZnS quantum dots: All-in-one theranostic nanomedicines with intrinsic fluorescence/photoacoustic phototherapy imaging for tumor, ACS Nano 10 (2016) 9637–9645. http://dx.doi.10.1021/acsnano.6b05419.
[85] W. Van Der Stam, A.C. Berends, C. De Mello, Prospects of colloidal copper chalcogenide nanocrystals, Chem. Phys. Chem. 17 (2016) 559–581. http://dx.doi.org/10.1002/cphc.201500976.
[86] K. Bi, N. Sui, L. Zhang, Y. Wang, Q. Liu, M. Tan, Q. Zhou, H. Zhang, Charge carrier dynamics investigation of CuInS2 quantum dots films using injected charge extraction by linearly increasing voltage (i-CELIV): the role of ZnS Shell, J. Nanopart. Res. 1 (2016) 8. http://dx.doi.org/10.1007/s11051-016-3635-3.
[87] J. Song, C. Ma, W. Zhang, S. Yang, S. Wang, L. Lv, L. Zhu, R. Xia, X. Xu, Tumor cell-targeted Zn_3 In_2 S_6 and Ag–Zn–In–S quantum dots for color adjustable luminophores, J. Mater. Chem. B 4 (2016) 7909–7918. http://dx.doi.org/10.1039/C6TB02297A.
[88] Z. Tan, Y. Zhang, C. Xie, H. Su, J. Liu, C. Zhang, N. Dellas, S.E. Mohney, Y. Wang, J. Wang, J. Xu, Near-band-edge electroluminescence from heavy-metal-free colloidal quantum dots, Adv. Mater. 23 (2011) 3553–3558. http://dx.doi.org/10.1002/adma.201100719.
[89] J. Song, C. Ma, W. Zhang, S. Yang, S. Wang, L. Lv, L. Zhu, R. Xia, X. Xu, Tumor cell-targeted Zn_3 In_2 S_6 and Ag–Zn–In–S quantum dots for color adjustable luminophores, J. Mater. Chem. B 4 (2016) 7909–7918. http://dx.doi.org/10.1039/C6TB02297A.
[90] H. Zhong, Z. Bai, B. Zou, Tuning the luminescence properties of colloidal I — III — VI semiconductor nanocrystals for optoelectronics and biotechnology applications, J. Phys. Chem. Lett. 3 (2012) 3167–3175. http://dx.doi.org/10.1021/jz301345x.
[91] D. Bera, L. Qian, T.K. Tseng, P.H. Holloway, Quantum dots and their multimodal applications: A review, Materials (Basel) 3 (2010) 2260–2345. http://dx.doi.org/10.3390/ma3042260.
[92] R.C. Fitzmorris, R.P. Oleksak, Z. Zhou, B.D. Mangum, J.N. Kurtin, G.S. Herman, Structural and optical characterization of CuInS 2 quantum dots synthesized by microwave-assisted continuous flow methods, J. Nanopart. Res. (2015) 1–10. http://dx.doi.org/10.1007/s11051-015-3123-1.
[93] J.-Y. Chang, G.-R. Chen, J.-D. Li, Synthesis of magnetofluorescence Gd-doped $CuInS_2$ /ZnS quantum dots with enhanced longitudinal relaxivity, Phys. Chem. Chem. Phys. 18 (2016) 7132–7140. http://dx.doi.org/10.1039/C5CP07063E.
[94] J.S. Steckel, B.K.H. Yen, D.C. Oertel, M.G. Bawendi, On the mechanism of lead chalcogenide nanocrystal formation, J. Am. Chem. Soc. 128 (2006) 13032–13033. http://dx.doi.org/10.1021/ja062626g.
[95] N. Chen, S. Cheng, C. Liu, J.S. Souris, C. Chen, Recent Advances in Nanoparticle-Based Förster Resonance Energy Transfer for Biosensing, Molecular Imaging and Drug Release Profiling (2012) 16598–16623. http://dx.doi.org/10.3390/ijms131216598.
[96] S. Krajewski, R. Prucek, A. Panacek, M. Avci-adali, A. Nolte, A. Straub, R. Zboril, H.P. Wendel, L. Kvitek, Acta Biomaterialia Hemocompatibility evaluation of different silver nanoparticle concentrations employing a modified Chandler-loop in vitro assay on human blood, ACTA Biomater. (2013). http://dx.doi.org/10.1016/j.actbio.2013.03.016.
[97] M. Helle, E. Cassette, L. Bezdetnaya, T. Pons, Visualisation of sentinel lymph node with indium-based near infrared emitting quantum dots in a murine metastatic breast cancer model, PLoS ONE 7 (2012) 7. http://dx.doi.org/10.1371/journal.pone.0044433.
[98] C.W. Chen, D.Y. Wu, Y.C. Chan, C.C. Lin, P.H. Chung, M. Hsiao, R.S. Liu, Evaluations of the chemical stability and cytotoxicity of CuInS2 and CuInS2/ZnS core/shell quantum dots, J. Phys. Chem. C 119 (2015) 2852–2860. http://dx.doi.org/10.1021/jp510908f.
[99] E. Hemmer, A. Benayas, F. Légaré, F. Vetrone, Exploiting the biological windows: current perspectives on fluorescent bioprobes emitting above 1000 nm, Nanoscale Horiz. 1 (2016) 168–184. http://dx.doi.org/10.1039/C5NH00073D.
[100] B. Cichy, A. Bednarkiewicz, W. Strek, Cadmium-free CuInS 2 quantum dots–candidate for bio-imaging applications, (n.d.), 54–66.
[101] T.A. Debele, S. Peng, H.C. Tsai, Drug carrier for photodynamic cancer therapy, Int. J. Mol. Sci. 16 (2015) 22094-22136. http://dx.doi.org/10.3390/ijms160922094.
[102] M. Zhao, B. Zhu, The Research and Applications of Quantum Dots as Nano-Carriers for Targeted Drug Delivery and Cancer Therapy, Nanoscale Res. Lett. (2016). http://dx.doi.org/10.1186/s11671-016-1394-9.
[103] X. Gao, Z. Liu, Z. Lin, X. Su, CuInS2 quantum dots/poly(l-glutamic acid)–drug conjugates for drug delivery and cell imaging, Analyst 139 (2014) 831. http://dx.doi.org/10.1039/c3an01134h.
[104] E. Blanco, H. Shen, M. Ferrari, Perspective principles of nanoparticle design for overcoming biological barriers to drug delivery, Nat. Biotechnol. 33 (2015) 941–951. http://dx.doi.org/10.1038/nbt.3330.
[105] E.C. Wang, A.Z. Wang, Nanoparticles and their applications in cell and molecular biology, Integr. Biol. 6 (2014) 9–26. http://dx.doi.org/10.1039/C3IB40165K.
[106] B. Xie, R. Hu, X. Luo, Quantum Dots-Converted Light-Emitting Diodes Packaging for Lighting and Display: Status and Perspectives, J. Electron. Package 138 (2016) 20803. http://dx.doi.org/10.1115/1.4033143.
[107] Z. Bai, W. Ji, D. Han, L. Chen, H. Shen, B. Zou, H. Zhong, Hydroxyl-terminated CuInS2 based quantum dots: Towards efficient and bright light emitting diodes, Chem. Mater. 1 (2016). http://dx.doi.org/10.1021/acs.chemmater.5b04480.
[108] F. Meinardi, H. McDaniel, F. Carulli, A. Colombo, K.A. Velizhanin, N.S. Makarov, R. Simonutti, V.I. Klimov, S. Brovelli, Highly efficient large-area colourless luminescent solar concentrators using heavy-metal-free colloidal quantum dots, Nat. Nanotechnol. 10 (2015) 878–885. http://dx.doi.org/10.1038/nnano.2015.178.
[109] A.R. Uhl, J.K. Katahara, H.W. Hillhouse, Environmental science, Energy Environ. Sci. 9 (2015) 130–134. http://dx.doi.org/10.1039/C5EE02870A.
[110] S.M. Kobosko, D.H. Jara, P.V. Kamat, AgInS 2 — ZnS quantum dots: Excited state interactions with TiO2 and photovoltaic performance, ACS Appl. Mater. Interfaces (2017). http://dx.doi.org/10.1021/acsami.6b14604.
[111] Y.-K. Kim, S.-H. Ahn, K. Chung, Y.-S. Cho, C.-J. Choi, The photoluminescence of $CuInS_2$ nanocrystals: effect of non-stoichiometry and surface modification, J. Mater. Chem. 22 (2012) 1516–1520. http://dx.doi.org/10.1039/C1JM13170B.
[112] S. Cao, C. Li, L. Wang, M. Shang, G. Wei, J. Zheng, W. Yang, Emissions in CuInS-ZnS quantum dots, Sci. Rep. (2014) 1–8. http://dx.doi.org/10.1038/srep07510.